ORIGINAL ARTICLE

WILEY

Upregulation of cadherin-11 contributes to cholestatic liver fibrosis

Bo Wu[1,2,3] (ORCID) | Xinbei Tian[1,2,3] | Weipeng Wang[1,2,3] | Jing Zhu[1,2,3] | Ying Lu[2,3] | Jun Du[2,3] | Yongtao Xiao[1,2,3]

[1]Department of Pediatric Surgery, Xin Hua Hospital, School of Medicine, Shanghai Jiao Tong University, Shanghai, China
[2]Department of Pediatric Gastroenterology and Nutrition, Shanghai Institute of Pediatric Research, Shanghai, China
[3]Shanghai Key Laboratory of Pediatric Gastroenterology and Nutrition, Shanghai, China

Correspondence
Yongtao Xiao, Department of Pediatric Surgery, Xin Hua Hospital, School of Medicine, Shanghai Jiao Tong University, No. 1665, Kong Jiang Road, Shanghai 200092, China.
Email: xiaoyongtao@xinhuamed.com.cn

ABSTRACT

Importance: Cadherin-11 (CDH11), a cell-to-cell adhesion molecule, is implicated in the fibrotic process of several organs. Biliary atresia (BA) is a common cholestatic liver disease featuring cholestasis and progressive liver fibrosis in children. Cholestatic liver fibrosis may progress to liver cirrhosis and lacks effective therapeutic strategies. Currently, the role of CDH11 in cholestatic liver fibrosis remains unclear.

Objective: This study aimed to explore the functions of CDH11 in cholestatic liver fibrosis.

Methods: The expression of *CDH11* in BA livers was evaluated by database analysis and immunostaining. Seven BA liver samples were used for immunostaining. The wild type (Wt) and *CDH11* knockout (*CDH11*$^{-/-}$) mice were subjected to bile duct ligation (BDL) to induce cholestatic liver fibrosis. The serum biochemical analysis, liver histology, and western blotting were used to assess the extent of liver injury and fibrosis as well as activation of transforming growth factor-β (TGF-β)/Smad pathway. The effect of CDH11 on the activation of hepatic stellate cell line LX-2 cells was investigated.

Results: Analysis of public RNA-seq datasets showed that *CDH11* expression levels were significantly increased in livers of BA, and CDH11 was correlated with liver fibrosis in BA. BDL-induced liver injury and liver fibrosis were attenuated in *CDH11*$^{-/-}$ mice compared to Wt mice. The protein expression levels of phosphorylated Smad2/3 were decreased in livers of *CDH11*$^{-/-}$ BDL mice compared to Wt BDL mice. *CDH11* knockdown inhibited the activation of LX-2 cells.

Interpretation: CDH11 plays an important role in cholestatic liver fibrosis and may represent a potential therapeutic target for cholestatic liver disease, such as BA.

KEYWORDS
Cadherin-11, Biliary atresia, Cholestatic liver fibrosis, TGF-β/Smad

INTRODUCTION

Cadherins are a group of Ca^{2+}-dependent transmembrane proteins that are principally located in adherent junctions and play roles in mediating homophilic cell-to-cell adhesion.[1–3] Cadherin-11 (CDH11) is an important member of the cadherin superfamily.[4] CDH11 is expressed in many cell types, such as osteoblasts, smooth muscle cells, mesenchymal stem cells, and fibroblasts.[5] In addition to mediating homophilic cellular adhesion, CDH11 also can regulate other biological functions, including cell proliferation, cell migration, cell differentiation, and tissue morphogenesis.[6,7] Dysregulated expression of CDH11 has been shown to be associated with several pathologic processes, such as fibrosis, inflammation, and tumor.[2,7,8] Moreover, CDH11 is expressed in many kinds of cells involved in the development of fibrosis, including fibroblasts, myofibroblasts, and macrophages.[7] Recent studies have shown that CDH11 plays crucial roles in pulmonary fibrosis, intestinal fibrosis, atrial fibrosis, and liver fibrosis induced by carbon tetrachloride (CCl_4).[6,7,9–11] Importantly, it is reported that CDH11 can mediate the profibrotic response in activated hepatic stellate cells (HSCs).[11] CDH11 is upregulated in transforming growth factor-$\beta1$ (TGF-$\beta1$) activated HSCs and contributes to the proliferation of HSCs.[11] However, whether CDH11 is involved in cholestatic liver fibrosis remains unclear.

Biliary atresia (BA) is a common cholestatic liver disease in children. BA is primarily caused by obliteration of the intrahepatic and extrahepatic biliary duct featuring cholestasis and progressive liver fibrosis.[12,13] In BA, cholestatic liver fibrosis may progress rapidly to liver cirrhosis and endanger children's life.[14] Kasai portoenterostomy is regarded as a first-line treatment choice for BA and it can rebuild bile flow from the liver to the intestine.[15] Although the Kasai portoenterostomy has improved the prognosis of BA, BA is still the major cause of liver transplantation in children.[16,17] Liver fibrosis is a pathological scarring process of liver damage.[14] The process of liver fibrosis is initiated when the growth factors, especially transforming growth factor-β (TGF-β), are synthesized and secreted under the stimulation of liver injury.[18] TGF-β can activate some cell types, including HSCs and portal fibroblasts (PFs), to produce extracellular matrix (ECM) proteins and contribute to liver fibrosis.[18] To date, the effective intervention of progressive liver fibrosis is still lacking. Finding effective therapeutic targets for cholestatic liver fibrosis is particularly important and urgent.

In the present study, we evaluated the expression of CDH11 in livers of BA and examined the role of CDH11 in cholestatic liver fibrosis by using *CDH11* knockout (*CDH11$^{-/-}$*) mice, bile duct ligation (BDL) mouse model, and hepatic stellate cell line LX-2 cells. Our findings indicate that CDH11 plays a critical role in promoting cholestatic liver fibrosis and targeting CDH11 may act as a potential therapeutic strategy for cholestatic liver disease, such as BA.

METHODS

Ethical approval

The analysis of liver specimens was approved by the Faculty of Medicine's Ethics Committee of Xin Hua Hospital, School of Medicine, Shanghai Jiao Tong University (XHEC-D-2021-080). All patients' guardians provided informed consent. The experiments with mice were approved by the Shanghai Jiao Tong University School of Medicine affiliated Xin Hua Hospital Animal Care and Use Committee (XHEC-F-2021-074). All procedures were performed following institutional guidelines for ethical animal studies and animal research laws.

Database analysis

For analysis of *CDH11* expression in BA patients, the public genomic dataset from Gene Expression Omnibus (GEO) database was used. The dataset discussed in the current study is derived from Bessho et al.[19] and accessible through GEO accession number GSE46995. The dataset includes a comprehensive gene expression profile of human livers from patients with BA ($n = 64$) and intrahepatic cholestasis (serving as diseased controls, referred to as NHS, neonatal hepatitis syndrome) ($n = 14$) and normal control subjects ($n = 7$).

Human liver specimens

A total of seven liver samples were retrieved from BA patients who underwent operations. These liver specimens were analyzed by immunohistochemistry and immunofluorescence to evaluate the expression of CDH11. Detailed clinical information of the BA patients was listed in Table S1.

BDL mouse model

CDH11$^{-/-}$ mice (Jackson Laboratory, Stock No: 023494) and wild type (Wt) mice with C57/BL6 background were housed under a 12-h light/dark cycle and fed standard food and tap water. Both *CDH11$^{-/-}$* and Wt mice (male and female, equal sex ratio, 6–8 weeks, $n = 6–8$) were subjected to BDL or sham operation as described previously.[20] Briefly, the mice were anesthetized with an intraperitoneal injection of pentobarbital sodium (1%) in a dosage of 7 μl/g body weight. After midline laparotomy, the common bile duct of mice was exposed and ligated with a 5–0 suture. The sham mice underwent a similar laparotomy without BDL. And the fascia was closed with a 6–0 suture, and the skin was then sutured with a 5–0 suture. After 2 or 4 weeks, the

mice were sacrificed for the next experiments. The serum samples were separated by centrifuging at 3800 rpm for 20 min at room temperature (RT) and were stored in a −80°C freezer before being used for biochemical analysis.

Quantitative real-time polymerase chain reaction

The quantitative real-time polymerase chain reaction was performed as previously described.[13] Briefly, total RNA was isolated from livers of mice using the RNeasy kit (Qiagen, Hilden, Germany) according to the manufacturer's instructions. The High Capacity cDNA Reverse Transcription kit (Applied Biosystems, Foster City, CA) was used to synthesize the cDNA. Then, we detected the mRNA expression levels of targeted genes by real-time PCR using PowerUp SYBR-Green Master Mix kit (Applied Biosystems, Foster City, CA) on the ViiA 7 Real-Time PCR System (Applied Biosystems). All samples were assayed in triplicate, and the data were normalized to endogenous control hypoxanthine phosphoribosyltransferase 1 (*Hprt1*). And relative gene quantities were obtained using the comparative cycle threshold method. The primer sequences were listed in Table S2.

Histology

The liver tissues from mice were fixed in 4% paraformaldehyde (Servicebio, Wuhan, China) for 24 h and went through dehydration, clearing, and paraffin embedding. Liver sections were cut at 4 μm thick and then mounted on positively charged slides, baked at 65°C for 1 h, and then stored at RT for later use. The liver biopsy samples were stained with hematoxylin and eosin, Masson's trichrome, and Sirius Red to evaluate the degree of liver fibrosis. The quantification of the fibrotic area of Masson's trichrome or Sirius Red staining images were performed as described previously.[21] Image J software (version 1.51k; National Institutes of Health, Bethesda, MD) was used to quantify the areas with Masson's trichrome or Sirius Red positive staining using 40 different fields (high magnification) from four animals of each group.

Immunohistochemistry analysis

Immunohistochemistry was performed using the diaminobenzidine chromogen method as described previously.[13] Briefly, paraffin-embedded tissues were deparaffinized by using xylol and descending concentrations of ethanol. Then, 0.3% H_2O_2 was used to block the endogenous peroxidases. After antigen retrieval with Citrate buffer, blocking was performed by using 5% bovine serum albumin (BSA). Then, incubation with primary antibodies against CDH11 (ab151302; Abcam, Cambridge, MA) was performed. The slides were rinsed in phosphate-buffered saline (PBS), and the slides were incubated with the secondary antibody (HRP conjugated goat antirab-bit IgG, GB23303; Servicebio) for 1 h at RT. Antibody binding was visualized by using a liquid DAB Substrate Chromogen System (Dako, Glostrup, Denmark). The slides were rinsed in PBS and then the slides were counterstained with hematoxylin.

Immunofluorescence staining

The immunofluorescence assays were performed using the methods described previously.[13,22] Briefly, the liver sections were incubated with xylol and descending concentrations of ethanol. The endogenous peroxidases were removed by using 0.3% H_2O_2. After blocking with 5% BSA, the CDH11, alpha-smooth muscle actin (α-SMA), and phosphorylated small mothers against decapentaplegic homolog 2 (p-Smad2) antibodies (CDH11, ab151302; Abcam, α-SMA, ab7817; Cambridge, MA, p-Smad2, 18338; Cell Signaling Technology, Danvers, MA) was applied overnight in a wet chamber. The secondary antibodies were applied to the slides for 1 h after washing three times with PBS at RT. The FITC conjugated goat antirab-bit IgG (GB22303; Servicebio), Cy3 conjugated goat anti-mouse IgG (GB21301; Servicebio), and Cy3 conjugated goat antirabbit IgG (GB21303; Servicebio) were used as secondary antibodies. Then, the nuclei were counterstained with 4′, 6-diamidino-2-phenylindole (DAPI). The positive staining signals were detected by fluorescent microscopy (Nikon, Tokyo, Japan).

Biochemical analysis

To assess the hepatic function of the mice, the serum alanine aminotransferase (ALT), aspartate aminotransferase (AST), γ-glutamyl transferase (GGT), alkaline phosphatase (AKP), total bilirubin (TBil), and direct bilirubin (DBil) levels were measured as per the manufacturer's instruction. Alanine aminotransferase assay kit (C009-2-1; Jiancheng, Nanjing, China), aspartate aminotransferase assay kit (C010-2-1; Jiancheng), γ-Glutamyl transferase assay kit (C017-2-1; Jiancheng), alkaline phosphatase assay kit (A059-2; Jiancheng), direct bilirubin kit (C019-2-1; Jiancheng) and total bilirubin kit (C019-1; Jiancheng) were used here.

Cell culture

The immortal human hepatic stellate cell line (LX-2) was obtained from China Cell Culture Center (Shanghai, China). The LX-2 cell line has been extensively used as a highly suitable model of human hepatic fibrosis due to its retaining key features of hepatic stellate cell and fibrogenesis. The LX-2 cells were cultured in Dulbecco's modified Eagle's medium (DMEM) at 37°C in an atmosphere of 5% carbon dioxide. The DMEM was supplemented with 10% fetal bovine serum (FBS). DMEM and FBS were obtained from GIBCO (Los Angeles, CA). LX-2 cells

were planted the day before infection and grew to 50%–70% confluence. LX-2 cells were infected with lentivirus vectors containing shRNA sequences targeting *CDH11* (*shCDH11*) or control shRNA. The lentivirus shRNA vectors (*CDH11* shRNA, target against GCGTATACCAGATGTCTGTGTCAGAA) were obtained from Genomeditech (Shanghai, China).

5-Ethynyl-2′-deoxyuridine proliferative assay

For proliferative analysis, the 5-ethynyl-2′-deoxyuridine (EdU) proliferative assay was performed on the LX-2 cells with or without *CDH11* knockdown using the Cell-Light EdU Apollo567 In Vitro Kit (C10310-1, RiboBio, Guangzhou, China). Briefly, the cells were incubated with 50 μM EdU for 2 h. The cells were centrifuged and fixed in 4% paraformaldehyde fixation, incubated with glycine, washed with PBS, and then permeabilized with 0.5% Triton X-100. After PBS washing, the cells were incubated with Apollo staining solution for 30 min. Then, the cells were washed with PBS containing 0.5% Triton X-100 three times, followed by incubation with Hoechst for 10 min. Photographs of the cells were captured with a fluorescent microscope (Nikon), and the positive cells were counted.

Western blot

The western blots were performed as previously described.[22,23] Briefly, total protein lysates were extracted from the liver tissues or LX2 cells by using radioimmunoprecipitation buffer (Servicebio) supplemented with a protease inhibitor cocktail (Servicebio). The equal amounts of protein were separated on NuPAGE 10% Bis-Tris gels (Invitrogen, Carlsbad, CA). The protein was electrophoretically transferred to polyvinylidene difluoride membranes. After blocking the membranes in 5% nonfat milk for 1 h at RT, the membranes were incubated with the primary antibodies overnight at 4°C. After washing three times (10 min per time) with Tris-buffered saline containing 0.1% Tween-20, the membranes were incubated with secondary antibodies for 1 h at RT. And the signals were detected by using Pierce ECL Western Blotting Substrate (Thermo Fisher Scientific, Rockford, IL). The primary antibodies (CDH11, ab151302; Abcam, dilution, 1:1000; α-SMA, ab32575; Abcam, dilution, 1:1000; p-Smad2, 3108P; Cell Signaling Technology, dilution, 1:1000; p-Smad3, 9520P, Cell Signaling Technology, Danvers, MA, dilution, 1:1000; Smad2, 5339P, Cell Signaling Technology, Danvers, MA, dilution, 1:1000; Smad3, 9523P, Cell Signaling Technology, Danvers, MA, dilution, 1:1000; Collagen I; Abcam, dilution, 1:1000; CK19, GB11197, Servicebio, dilution, 1:1000; beta-actin, 4970S, Cell Signaling Technology, Danvers, MA, dilution, 1:1500; GAPDH, 5174, Cell Signaling Technology, dilution, 1:1000) were applied. The HRP-linked antirabbit IgG antibody (7074,

Cell Signaling Technology) and HRP-linked antimouse IgG antibody (7076, Cell Signaling Technology) were used as secondary antibodies. The relative protein levels were quantified by using the Image Lab software (version 3.0; Bio-Rad, Hercules, CA) according to the band gray value.

Statistical analysis

The results were analyzed by using GraphPad Prism (version 8.0; GraphPad Software Inc., San Diego, CA). Normally distributed data were expressed as mean ± standard deviation, and the statistical significance was determined using unpaired Student's *t*-test or one-way analysis of variance for comparisons of different groups. Non-normally distributed data were expressed as median (interquartile range), and statistical analysis was performed by using the Mann-Whitney *U* test or Kruskal-Wallis test. The correlation analysis was conducted by using Spearman correlation. *P*-value less than 0.05 represented statistical significance.

RESULTS

CDH11 was correlated with liver fibrosis in BA patients

Analysis of publicly available dataset (GSE46995 for human liver tissue) showed that *CDH11* expression levels were significantly increased in liver tissues from patients with BA compared to liver tissues from patients with NHS and normal liver tissues (Figure 1A).[19] Correlation analysis demonstrated that hepatic *CDH11* expression levels were positively correlated with expression levels of hepatic collagen type I alpha 1 (*COL1A1*; $r = 0.80$; $P < 0.0001$) and actin alpha 2, smooth muscle (*ACTA2*; $r = 0.66$; $P < 0.0001$) (Figure 1B).[19] We performed immunohistochemistry and immunofluorescence staining to further investigate the expression of CDH11 in livers of BA patients. The immunohistochemistry results showed that CDH11 was expressed in PFs in livers of BA patients (Figure 1C). Additionally, the results showed that CDH11 was detected in the fibrotic area where collagen I deposition and α-SMA expression were prominent in BA patients' livers (Figure 1D). Moreover, the results of immunofluorescence staining showed that CDH11 was detected in p-Smad2-positive cells in livers of BA patients (Figure 1D).

CDH11 knockout ameliorated BDL-induced liver injury in mice

The immunofluorescence analysis showed that the expression levels of CDH11 were increased in liver tissues from BDL mice compared to Sham mice (Figure S1A). Then we used *CDH11* knockout mice to further investigate the role of CDH11 *in vivo*. After 4-week BDL, the gross appearances of the livers or serum were more yellowish in Wt mice than *CDH11*$^{-/-}$ mice (Figure 2A).
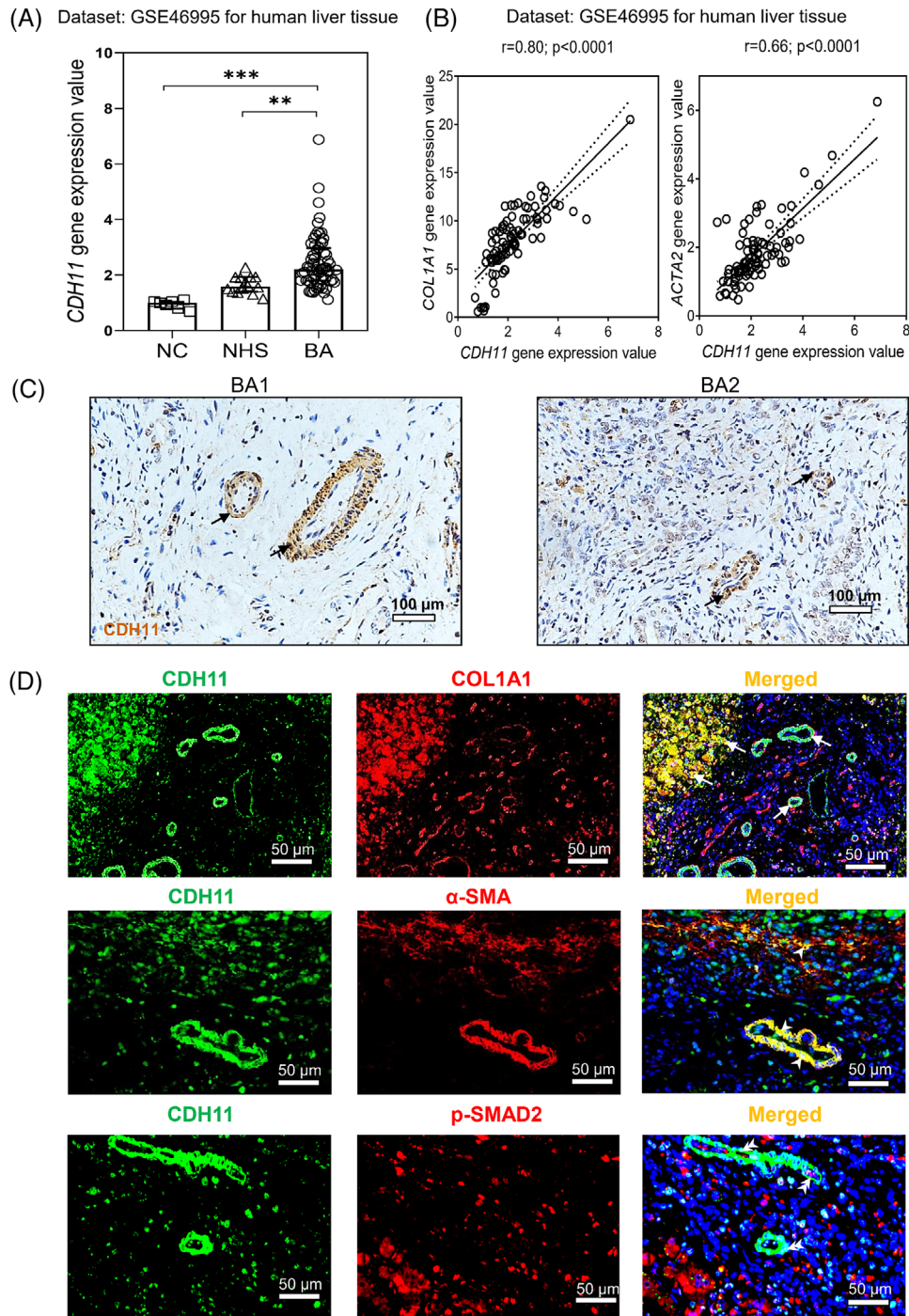
FIGURE 1 CDH11 was closely correlated with liver fibrosis in BA. (A) Data for *CDH11* mRNA expression extracted from the GEO database, comparing livers from patients with BA ($n = 64$) and NHS ($n = 14$) and normal control subjects ($n = 7$) (GSE46995). (B) Correlation analysis of *CDH11* expression level with *COL1A1* and *ACTA2*. Data extracted from the GEO database (GSE46995). (C) Representative immunohistochemistry images of CDH11 in livers of BA patients ($n = 4$). Scale bars: $100\,\mu$m. Black arrows indicate portal fibroblasts. (D) Representative images of immunofluorescence co-staining for CDH11 and COL1A1, CDH11 and α-SMA, CDH11 and p-Smad2 in livers of BA patients ($n = 3$). Scale bars: $50\,\mu$m. Arrows indicate CDH11/COL1A1 double-positive areas, arrowheads indicate CDH11/α-SMA double-positive myofibroblasts, and double-arrowheads indicate CDH11/p-Smad2 double-positive cells. Statistical significance: $**P < 0.01$, $***P < 0.001$. BA, biliary atresia; NHS, neonatal hepatitis syndrome; NC, normal controls; COL1A1, collagen type I alpha 1; α-SMA, alpha-smooth muscle actin; ACTA2, actin alpha 2, smooth muscle; p-Smad2, phosphorylated small mothers against decapentaplegic homolog 2.
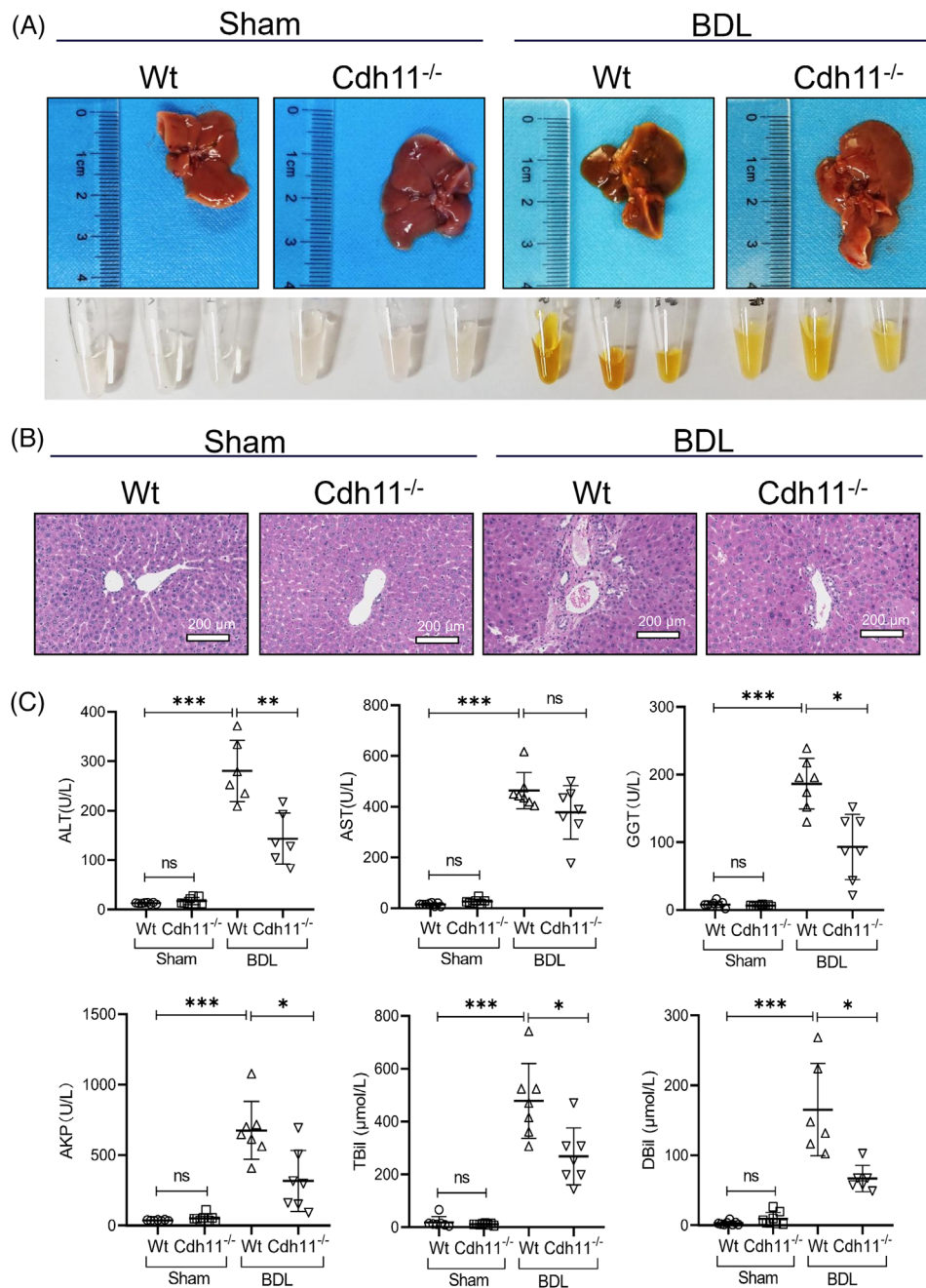
FIGURE 2 *Cdh11* deficiency reduced BDL-induced liver damage in mice. (A) The gross appearances of the livers and serum from Sham Wt, Sham *Cdh11*⁻/⁻, BDL Wt, and BDL *Cdh11*⁻/⁻ mice. Each group contains eight mice. (B) Representative images of Hematoxylin-eosin staining for livers of Sham Wt, Sham *Cdh11*⁻/⁻, BDL Wt, and BDL *Cdh11*⁻/⁻ mice. Scale bars: 200 μm. Images are representative of four mice from each group. (C) Measurement of serum ALT, AST, GGT, AKP, TBil, and DBil levels in Sham Wt, Sham *Cdh11*⁻/⁻, BDL Wt, and BDL *Cdh11*⁻/⁻ mice. Each group contains 6–8 mice. Statistical significance: *$P < 0.05$; **$P < 0.01$; ***$P < 0.001$; ns, not significant. The mice were subjected to a 4-week BDL or sham operation. *Cdh11*, cadherin-11; Wt, wild type; BDL, bile duct ligation; Sham, sham-operated; ALT, alanine aminotransferase; AST, aspartate aminotransferase; GGT, γ-glutamyl transferase; AKP, alkaline phosphatase; TBil, total bilirubin; DBil, direct bilirubin.

Hematoxylin-eosin (H&E) staining showed that BDL induced increased inflammatory cell infiltration in livers of Wt BDL mice, but BDL had much less impact in *CDH11*⁻/⁻ BDL mice (Figure 2B). The results of the biochemical analysis showed that serum ALT, AST, GGT, AKP, TBil, and DBil levels were significantly increased in Wt BDL mice compared to Wt Sham mice, but decreased in *CDH11*⁻/⁻ BDL mice compared to Wt BDL mice (Figure 2C).

CDH11 deficiency attenuated BDL-induced liver fibrosis in mice

After 2-week BDL, co-immunofluorescent staining of CDH11 (green) and α-SMA (red) showed that there were some dual staining CDH11+/α-SMA+ myofibroblasts in livers of BDL mice (Figure S1B). Moreover, the results showed that there was a less fibrotic area in livers of *CDH11*$^{-/-}$ BDL mice than Wt BDL mice (Figure S2A). The mRNA levels of transforming growth factor-beta 1 (*Tgfb1*) and cyclin D1 (*Ccnd1*) were significantly decreased in livers of *CDH11*$^{-/-}$ BDL mice relative to that of Wt BDL mice (Figure S2B). In addition, the mRNA levels of fibulin (*Fbln*), mesothelin (*Msln*), thymus cell antigen 1 (*Thy1*), *ACTA2, COL1A1*, and tissue inhibitor of metalloproteinases 1 (*Timp1*) were also decreased in *CDH11*$^{-/-}$ BDL mice, but these were not statistically significant (Figure S2B). After 4-week BDL or sham operation, the results of Sirius Red staining and Masson's trichrome staining indicated that BDL significantly induced liver fibrosis in Wt mice, but had much less effects on *CDH11*$^{-/-}$ mice (Figure 3A–C). At a molecular level, the expression levels of collagen I, α-SMA, and cytokeratin 19 (CK19) were decreased in livers of *CDH11*$^{-/-}$ BDL mice compared to Wt BDL mice, as shown by western blot analysis (Figure 3D–E).

CDH11 depletion attenuated the TGF-β/Smad pathway in cholestatic livers

A TGF-β/Smad signaling pathway is identified as a crucial pathogenic pathway in tissue fibrosis.[24] In this study, the results of co-immunofluorescent staining showed that CDH11 was detected in p-Smad2-positive cells in livers of BDL mice (Figure S1B). Moreover, we evaluated the expression of several key proteins in the TGF-β/Smad signaling pathway in livers of Wt and *CDH11*$^{-/-}$ mice that underwent BDL or sham operation by western blotting. The results showed that after 4-week BDL or sham operation, the protein levels of phosphorylated small mothers against decapentaplegic homolog 2/3 (p-Smad2, p-Smad3) were significantly increased in Wt BDL mice compared with Wt Sham mice, while these proteins were reduced in *CDH11*$^{-/-}$ BDL mice compared to Wt BDL mice (Figure 3D–E).

CDH11 knockdown inhibited the activation of HSCs *in vitro*

Next, we further investigated the effect of *CDH11* on the activation of the hepatic stellate cell line LX-2 cells. The expression of *CDH11* was markedly downregulated in LX-2 cells infected with lentivirus vectors containing *shCDH11*, as shown by western blot analysis (Figure 4C). The results of the EdU proliferative assay showed that infection with lentivirus vectors containing *shCDH11* inhibited the proliferation of LX-2 cells compared to controls (Figure 4A–B). Moreover, knocking down *CDH11*

expression significantly suppressed the expression of α-SMA in LX-2 cells compared to controls (Figure 4C).

DISCUSSION

Liver fibrosis in cholestatic liver diseases, such as BA, may rapidly advance to liver cirrhosis, which often leads to liver failure and requires liver transplantation.[25,26] It is significant to explore the mechanisms and search for effective therapies for cholestatic liver fibrosis. CDH11, an important adhesion molecule, is implicated in several fibrotic diseases, including dermal fibrosis, pulmonary fibrosis, and CCl$_4$-induced liver fibrosis, but we don't know if CDH11 has any effect on cholestatic liver fibrosis.[1,6,7,11] In this study, we focused on the expression of CDH11 in livers of BA and the functions of CDH11 in cholestatic liver fibrosis. We found that CDH11 was correlated with liver fibrosis in BA, and upregulation of CDH11 contributed to cholestatic liver fibrosis.

BA is an important cholestatic liver disorder and the major indication for pediatric liver transplantation.[27] Cholestatic liver fibrosis is regarded as a prominent feature of BA. Using a public dataset, we showed that significantly higher expression levels of *CDH11* were observed in livers of BA patients compared to the control subjects, and *CDH11* expression levels were positively correlated with expression levels of liver fibrotic marker genes, including *COL1A1* and *ACTA2*. These findings indicated that *CDH11* was correlated with liver fibrosis in BA. It is reported that PFs are an important source of hepatic myofibroblasts and contribute to cholestatic liver fibrosis.[28] In our study, we showed that CDH11 was expressed in PFs and fibrotic areas of BA livers. Moreover, CDH11 was expressed in p-Smad2-positive cells in livers of BA patients. From the above results, we infer that CDH11 may play important roles in liver fibrosis in BA.

BDL is a widely used experimental model to induce cholestatic liver fibrosis.[20] In the current study, we used *CDH11* knockout mice and the BDL mouse model to further explore the role of CDH11 in cholestatic liver fibrosis. As expected, our results demonstrated that BDL markedly induced liver fibrosis in Wt mice, but BDL had much less induction in *CDH11*$^{-/-}$ mice. And *CDH11* knockout significantly decreased the expression levels of hepatic fibrosis-related proteins, including collagen I, α-SMA, and CK19, in livers of BDL mice. These results indicated that the knockout of *CDH11* could ameliorate BDL-induced liver fibrosis. Similarly, Pedroza et al.[10] have reported that *CDH11* deficiency can reduce liver fibrosis induced by CCl4. These findings suggest that CDH11 may be an important mediator of hepatic fibrosis. Liver fibrosis is an abnormal wound healing process and is characterized by excessive accumulation of ECM proteins.[25,29] Activation of HSCs has been shown to be the essential
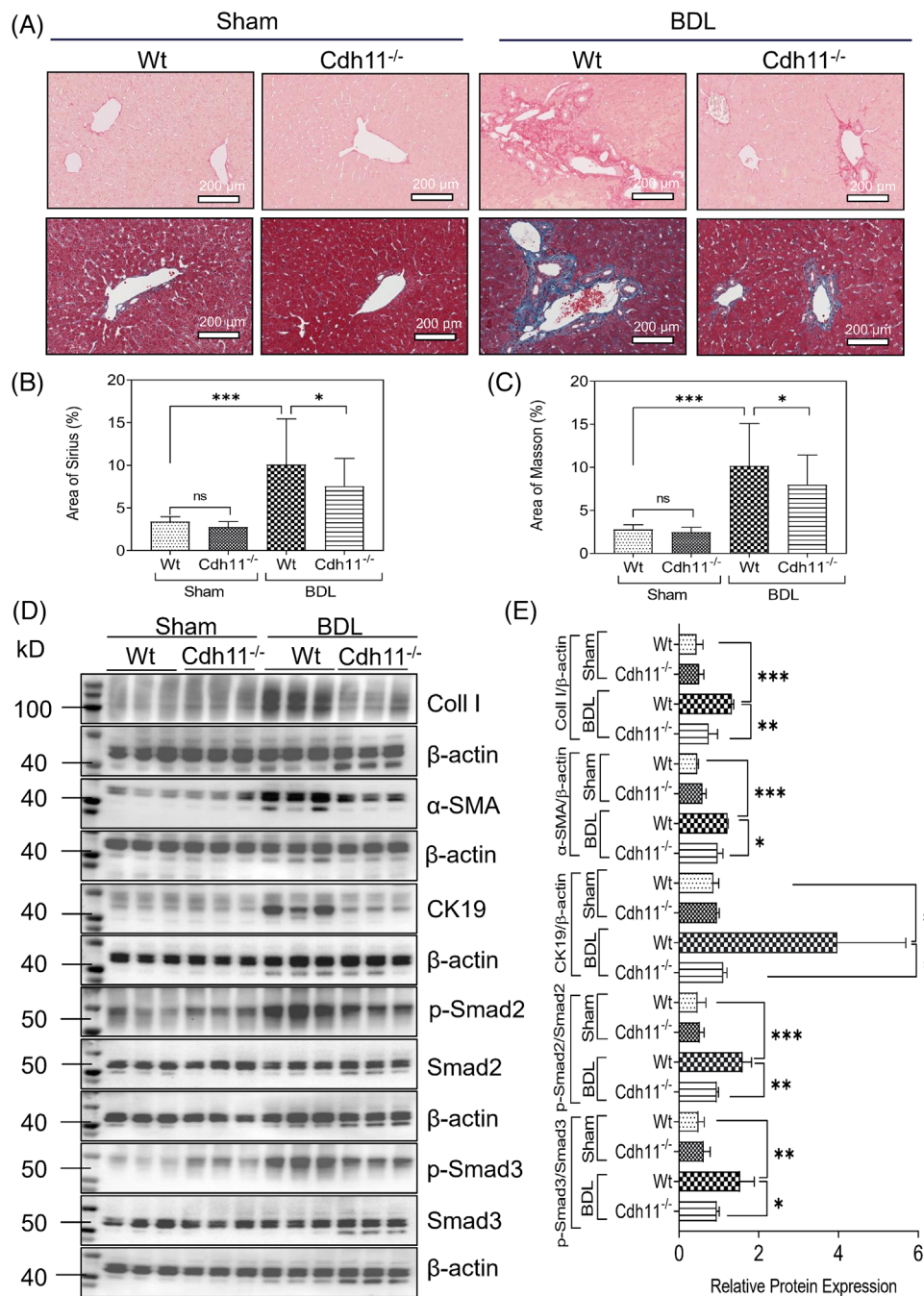
FIGURE 3 *Cdh11* knockout suppressed BDL-induced liver fibrosis in mice. (A) Representative images of Sirius Red staining and Masson's trichrome staining of Sham Wt, Sham *Cdh11*$^{-/-}$, BDL Wt, and BDL *Cdh11*$^{-/-}$ mice. Scale bars: 200 μm. (B, C) Quantification of the fibrotic area of Sirius Red staining images and Masson's trichrome staining images. Sham Wt ($n = 4$), Sham *Cdh11*$^{-/-}$ ($n = 4$), BDL Wt ($n = 4$), BDL *Cdh11*$^{-/-}$ ($n = 4$) mice. 40 fields (high magnification) were randomly selected from four mice of each group for quantification. (D) Western blot analysis for Coll I, α-SMA, CK19, p-Smad2, Smad2, p-Smad3, and Smad3 in livers of Sham Wt, Sham *Cdh11*$^{-/-}$, BDL Wt and BDL *Cdh11*$^{-/-}$ mice. Each group contains three mice. (E) Quantification of the panel (D). Statistical significance: *$P < 0.05$; **$P < 0.01$; ***$P < 0.001$; ns, not significant. The mice were subjected to a 4-week BDL or sham operation. *Cdh11*, cadherin-11; Wt, wild type; BDL, bile duct ligation; Sham, sham-operated; Coll I, collagen type I; α-SMA, alpha-smooth muscle actin; CK19, cytokeratin 19; Smad2, small mothers against decapentaplegic homolog 2; Smad3, small mothers against decapentaplegic homolog 3; p-Smad2, phosphorylated small mothers against decapentaplegic homolog 2; p-Smad3, phosphorylated small mothers against decapentaplegic homolog 3.
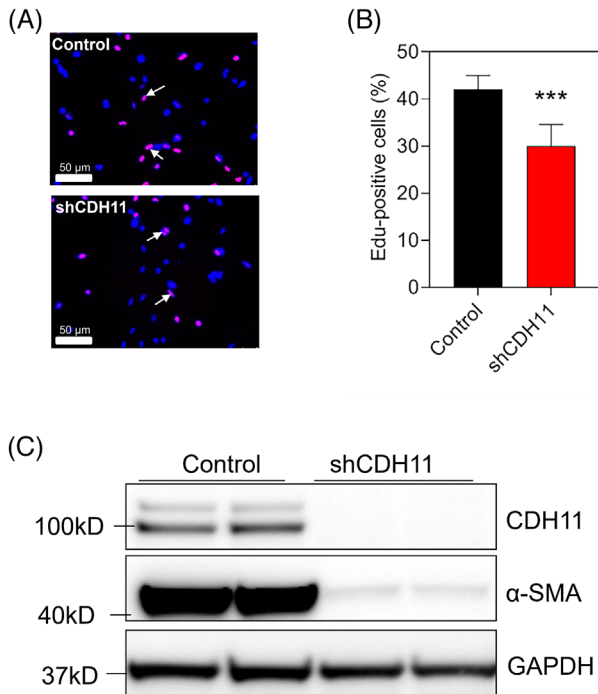
(A)

(B)

(C)

FIGURE 4 Knockdown of *CDH11* inhibited LX-2 cell activation. (A) The proliferation of LX-2 cells infected with lentivirus vectors containing *shCDH11* and controls was evaluated by EdU proliferative assay. Scale bars: 50 μm. Arrows indicate EdU-positive cells. (B) The percentage of EdU-positive cells was counted in LX-2 cells infected with lentivirus vectors containing *shCDH11* and controls. (C) Protein expression levels of CDH11 and α-SMA in LX-2 cells infected with lentivirus vectors containing *shCDH11* and controls were determined by western blot analysis. Statistical significance: ***$P < 0.001$. *CDH11*, cadherin-11; *shCDH11*, shRNA sequences targeting *CDH11*; α-SMA, alpha-smooth muscle actin; GAPDH, glyceraldehyde-3-phosphate dehydrogenase; EdU, 5-Ethynyl-2′-deoxyuridine.

event in liver fibrogenesis.[25,29,30] Indeed, it is reported that HSCs are the main contributors to cholestatic liver fibrosis and the major source of myofibroblasts in cholestatic liver fibrosis.[31,32] Ruan et al.[11] reported that CDH11 could promote the proliferation of LX-2 cells via the plate cloning experiments and CCK-8 assay. In this study, according to the results of western blot and EdU proliferative assay, we found that knocking down *CDH11* inhibited the activation of HSCs. These results indicated that CDH11 played important roles in the activation of HSCs. From the above findings, we could infer that CDH11 could promote the process of cholestatic liver fibrosis. It was reported that CDH11 blocking with a functional blocking antibody (SYN0012) reduced inflammation-driven fibrotic remodeling after myocardial infarction.[33] We believe that inhibitors or blocking antibodies of CDH11 are beneficial to liver fibrotic intervention in patients with cholestatic liver diseases, such as BA.

At the molecular level, the process of liver fibrosis is involved in the complex modulation of intracellular sig-

nal transduction. A TGF-β/Smad signaling pathway is regarded as a key profibrogenic pathway that can promote HSC activation as well as ECM production and plays crucial roles in liver fibrosis.[34,35] In this pathway, TGF-β ligand binds to TGF-β type II receptor (TβRII), and then TβRII forms a heterodimer with TGF-β type I receptor (TβRI), activating TβRI to phosphorylate Smad2 and Smad3 proteins.[36,37] The phosphorylated Smad2 and Smad3 form a complex with Smad4 protein, and the complex translocates to the nucleus to regulate the expression of profibrotic genes.[36–38] Recent studies indicated that CDH11 could enhance the activation of TGF-β/Smad signaling pathway in Angiotensin II-activated atrial fibroblasts and facilitate atrial fibrosis.[6] In addition, *CDH11* knockout reduced TGF-β signaling and dermal fibrosis in the mouse model of bleomycin-induced dermal fibrosis.[1] The current study demonstrated that CDH11 was expressed in p-Smad2-positive cells in livers of BDL mice, suggesting that CDH11 might be related to the TGF-β/Smad signaling in livers of BDL mice. Then, we found that knockout of *CDH11* significantly attenuated the expression levels of *Tgfb1* in livers of BDL mice, indicating that CDH11 may act as an upstream regulator of TGF-β1. Furthermore, we showed that activated Smad2/3 protein levels were markedly increased in livers under cholestatic conditions in Wt BDL mice, while they were reduced in *CDH11*$^{-/-}$ BDL mice. These results suggested that CDH11 might contribute to BDL-induced liver fibrosis by promoting the activation of the TGF-β/Smad signaling pathway.

In conclusion, this study demonstrates that there is a close relationship between CDH11 and cholestatic liver fibrosis. We propose that CDH11 plays important roles in cholestatic liver fibrosis may via regulating the TGF-β/Smad signaling pathway under cholestatic conditions. Our results suggest that CDH11 may act as a potential target to attenuate liver fibrosis in cholestatic liver diseases, such as BA. Still, there is a lot we don't know and much work that should be done. For example, the effects of CDH11 on HSCs and PFs and the specific mechanism in cholestatic liver fibrosis need further study in the future.

CONFLICT OF INTEREST

The authors declare that they have no conflict of interest.

REFERENCES

1. Wu M, Pedroza M, Lafyatis R, George AT, Mayes MD, Assassi S, et al. Identification of cadherin 11 as a mediator of dermal fibrosis and possible role in systemic sclerosis. *Arthritis Rheumatol.* 2014;66:1010-1021. DOI: 10.1002/art.38275
2. Chang SK, Noss EH, Chen M, Gu Z, Townsend K, Grenha R, et al. Cadherin-11 regulates fibroblast inflammation.

Proc Natl Acad Sci USA. 2011;108:8402-8407. DOI: 10. 1073/pnas.1019437108

3. Lee DM, Kiener HP, Agarwal SK, Noss EH, Watts GF, Chisaka O, et al. Cadherin-11 in synovial lining formation and pathology in arthritis. *Science.* 2007;315:1006-1010. DOI: 10.1126/science.1137306

4. Lee YC, Bilen MA, Yu G, Lin SC, Huang CF, Ortiz A, et al. Inhibition of cell adhesion by a cadherin-11 antibody thwarts bone metastasis. *Mol Cancer Res.* 2013;11:1401-1411. DOI: 10.1158/1541-7786.MCR-13-0108

5. Chen X, Xiang H, Yu S, Lu Y, Wu T. Research progress in the role and mechanism of Cadherin-11 in different diseases. *J Cancer.* 2021;12:1190-1199. DOI: 10.7150/jca.52720

6. Cao W, Song S, Fang G, Li Y, Wang Y, Wang QS. Cadherin-11 deficiency attenuates Ang-II-induced atrial fibrosis and susceptibility to atrial fibrillation. *J Inflamm Res.* 2021;14:2897-2911. DOI: 10.2147/JIR.S306073

7. Schneider DJ, Wu M, Le TT, Cho SH, Brenner MB, Blackburn MR, et al. Cadherin-11 contributes to pulmonary fibrosis: potential role in TGF-β production and epithelial to mesenchymal transition. *FASEB J.* 2012;26:503-512. DOI: 10.1096/fj.11-186098

8. Birtolo C, Pham H, Morvaridi S, Chheda C, Go VL, Ptasznik A, et al. Cadherin-11 is a cell surface marker up-regulated in activated pancreatic stellate cells and is involved in pancreatic cancer cell migration. *Am J Pathol.* 2017;187:146-155. DOI: 10.1016/j.ajpath.2016.09.012

9. Franzè E, Monteleone I, Laudisi F, Rizzo A, Dinallo V, Di Fusco D, et al. Cadherin-11 is a regulator of intestinal fibrosis. *J Crohns Colitis.* 2020;14:406-417. DOI: 10.1093/ecco-jcc/jjz147

10. Pedroza M, To S, Smith J, Agarwal SK. Cadherin-11 contributes to liver fibrosis induced by carbon tetrachloride. *PLoS One.* 2019;14:e0218971. DOI: 10.1371/journal.pone. 0218971

11. Ruan W, Pan R, Shen X, Nie Y, Wu Y. CDH11 promotes liver fibrosis via activation of hepatic stellate cells. *Biochem Biophys Res Commun.* 2019;508:543-549. DOI: 10.1016/j. bbrc.2018.11.153

12. Feldman AG, Mack CL. Biliary atresia: cellular dynamics and immune dysregulation. *Semin Pediatr Surg.* 2012;21:192-200. DOI: 10.1053/j.sempedsurg.2012.05.003

13. Xiao Y, Liu R, Li X, Gurley EC, Hylemon PB, Lu Y, et al. Long noncoding RNA H19 contributes to cholangiocyte proliferation and cholestatic liver fibrosis in biliary atresia. *Hepatology.* 2019;70:1658-1673. DOI: 10.1002/hep.30698.

14. El-Araby HA, Saber MA, Radwan NM, Taie DM, Adawy NM, Sira AM. SOX9 in biliary atresia: new insight for fibrosis progression. *Hepatobiliary Pancreat Dis Int.* 2021;20:154-162. DOI: 10.1016/j.hbpd.2020.12.007

15. Du M, Wang J, Tang Y, Jiang J, Chen G, Huang Y, et al. Evaluation of perioperative complications in the management of biliary atresia. *Front Pediatr.* 2020;8:460. DOI: 10. 3389/fped.2020.00460

16. Okubo R, Nio M, Sasaki H. Japanese Biliary Atresia Society. Impacts of early Kasai portoenterostomy on short-term and long-term outcomes of biliary atresia. *Hepatol Commun.* 2021;5:234-243. DOI: 10.1002/hep4.1615

17. Zhou K, Xie G, Wen J, Wang J, Pan W, Zhou Y, et al. Histamine is correlated with liver fibrosis in biliary atresia. *Dig Liver Dis.* 2016;48:921-926. DOI: 10.1016/j.dld.2016. 05.001

18. Sigal M, Siebert N, Zechner D, Menschikow E, Abshagen K, Vollmar B, et al. Darbepoetin-α inhibits the perpetuation of necro-inflammation and delays the progression of cholestatic fibrosis in mice. *Lab Invest.* 2010;90:1447-1456. DOI: 10. 1038/labinvest.2010.115

19. Bessho K, Mourya R, Shivakumar P, Walters S, Magee JC, Rao M, et al. Gene expression signature for biliary atresia and a role for interleukin-8 in pathogenesis of experimental disease. *Hepatology.* 2014;60:211-223. DOI: 10.1002/hep. 27045

20. Tag CG, Sauer-Lehnen S, Weiskirchen S, Borkham-Kamphorst E, Tolba RH, Tacke F, et al. Bile duct ligation in mice: induction of inflammatory liver injury and fibrosis by obstructive cholestasis. *J Vis Exp.* 2015. DOI: 10.3791/ 52438

21. Hartmann P, Haimerl M, Mazagova M, Brenner DA, Schnabl B. Toll-like receptor 2-mediated intestinal injury and enteric tumor necrosis factor receptor I contribute to liver fibrosis in mice. *Gastroenterology.* 2012;143:1330-1340. DOI: 10. 1053/j.gastro.2012.07.099

22. Wan X, Tian X, Du J, Lu Y, Xiao Y. Long non-coding RNA H19 deficiency ameliorates bleomycin-induced pulmonary inflammation and fibrosis. *Respir Res.* 2020;21:290. DOI: 10.1186/s12931-020-01534-6

23. Xiao Y, Wang J, Yan W, Zhou Y, Chen Y, Zhou K, et al. Dysregulated miR-124 and miR-200 expression contribute to cholangiocyte proliferation in the cholestatic liver by targeting IL-6/STAT3 signalling. *J Hepatol.* 2015;62:889-896. DOI: 10.1016/j.jhep.2014.10.033

24. Hu HH, Chen DQ, Wang YN, Feng YL, Cao G, Vaziri ND, et al. New insights into TGF-beta/Smad signaling in tissue fibrosis. *Chem Biol Interact.* 2018;292:76-83. DOI: 10.1016/ j.cbi.2018.07.008

25. Xiao Y, Wang J, Chen Y, Zhou K, Wen J, Wang Y, et al. Up-regulation of miR-200b in biliary atresia patients accelerates proliferation and migration of hepatic stallate cells by activating PI3K/Akt signaling. *Cell Signal.* 2014;26:925-932. DOI: 10.1016/j.cellsig.2014.01.003

26. Fenlon M, Short C, Xu J, Malkoff N, Mahdi E, Hough M, et al. Prominin-1-expressing hepatic progenitor cells induce fibrogenesis in murine cholestatic liver injury. *Physiol Rep.* 2020;8:e14508. DOI: 10.14814/phy2.14508

27. Haafiz AB. Liver fibrosis in biliary atresia. *Expert Rev Gastroenterol Hepatol.* 2010;4:335-343. DOI: 10.1586/egh.10. 29

28. Iwaisako K, Jiang C, Zhang M, Cong M, Moore-Morris TJ, Park TJ, et al. Origin of myofibroblasts in the fibrotic liver in mice. *Proc Natl Acad Sci USA.* 2014;111:E3297-3305. DOI: 10.1073/pnas.1400062111

29. Xiang D, Zou J, Zhu X, Chen X, Luo J, Kong L, et al. Physalin D attenuates hepatic stellate cell activation and liver fibrosis by blocking TGF-β/Smad and YAP signaling. *Phytomedicine.* 2020;78:153294. DOI: 10.1016/j.phymed.2020. 153294

30. Friedman SL. Mechanisms of disease: mechanisms of hepatic fibrosis and therapeutic implications. *Nat Clin Pract Gastroenterol Hepatol.* 2004;1:98-105. DOI: 10.1038/ncpgasthep0055

31. Liu R, Li X, Zhu W, Wang Y, Zhao D, Wang X, et al. Cholangiocyte-derived exosomal long noncoding RNA H19 promotes hepatic stellate cell activation and cholestatic liver fibrosis. *Hepatology.* 2019;70:1317-1335. DOI: 10.1002/hep.30662

32. Mederacke I, Hsu CC, Troeger JS, Huebener P, Mu X, Dapito DH, et al. Fate tracing reveals hepatic stellate cells as dominant contributors to liver fibrosis independent of its aetiology. *Nat Commun.* 2013;4:2823. DOI: 10.1038/ncomms3823

33. Schroer AK, Bersi MR, Clark CR, Zhang Q, Sanders LH, Hatzopoulos AK, et al. Cadherin-11 blockade reduces inflammation-driven fibrotic remodeling and improves outcomes after myocardial infarction. *JCI Insight.* 2019;4. DOI: 10.1172/jci.insight.131545

34. Xu S, Mao Y, Wu J, Feng J, Li J, Wu L, et al. TGF-β/Smad and JAK/STAT pathways are involved in the anti-fibrotic effects of propylene glycol alginate sodium sulphate on hepatic fibrosis. *J Cell Mol Med.* 2020;24:5224-5237. DOI: 10.1111/jcmm.15175

35. Yan Y, Zeng J, Xing L, Li C. Extra- and intra-cellular mechanisms of hepatic stellate cell activation. *Biomedicines.* 2021;9. DOI: 10.3390/biomedicines9081014

36. Shi Y, Massagué J. Mechanisms of TGF-beta signaling from cell membrane to the nucleus. *Cell.* 2003;113:685-700. DOI: 10.1016/s0092-8674(03)00432-x

37. Massagué J. TGFβ signalling in context. *Nat Rev Mol Cell Biol.* 2012;13:616-630. DOI: 10.1038/nrm3434

38. Xu F, Liu C, Zhou D, Zhang L. TGF-beta/SMAD pathway and its regulation in hepatic fibrosis. *J Histochem Cytochem.* 2016;64:157-167. DOI: 10.1369/0022155415627681

SUPPORTING INFORMATION

Additional Supporting Information may be found online in the supporting information tab for this article.